

MIT Open Access Articles

Enhanced external quantum efficiency in an organic photovoltaic cell via singlet fission exciton sensitizer

The MIT Faculty has made this article openly available. **Please share** how this access benefits you. Your story matters.

Citation: Reuswig, P. D., D. N. Congreve, N. J. Thompson, and M. A. Baldo. "Enhanced External Quantum Efficiency in an Organic Photovoltaic Cell via Singlet Fission Exciton Sensitizer." Appl. Phys. Lett. 101, no. 11 (2012): 113304. © 2012 American Institute of Physics

As Published: <http://dx.doi.org/10.1063/1.4752445>

Publisher: American Institute of Physics (AIP)

Persistent URL: <http://hdl.handle.net/1721.1/85957>

Version: Final published version: final published article, as it appeared in a journal, conference proceedings, or other formally published context

Terms of Use: Article is made available in accordance with the publisher's policy and may be subject to US copyright law. Please refer to the publisher's site for terms of use.



Enhanced external quantum efficiency in an organic photovoltaic cell via singlet fission exciton sensitizer

P. D. Reuswig, D. N. Congreve, N. J. Thompson, and M. A. Baldo

Citation: [Applied Physics Letters](#) **101**, 113304 (2012); doi: 10.1063/1.4752445

View online: <http://dx.doi.org/10.1063/1.4752445>

View Table of Contents: <http://scitation.aip.org/content/aip/journal/apl/101/11?ver=pdfcov>

Published by the [AIP Publishing](#)

The advertisement features a central image of the Model PS-100 probe station, a complex piece of scientific equipment with various lenses, stages, and sensors. The background is a gradient from light blue to dark blue. On the left, the text 'NEW Model PS-100 Preconfigured Tabletop Probe Station' is written in white and orange. On the right, the 'Lake Shore CRYOTRONICS' logo is shown, with the tagline 'An affordable solution for a wide range of research' below it.

NEW
Model PS-100
Preconfigured Tabletop
Probe Station

Lake Shore
CRYOTRONICS

*An affordable solution for
a wide range of research*

Enhanced external quantum efficiency in an organic photovoltaic cell via singlet fission exciton sensitizer

P. D. Reuswig,^{1,a)} D. N. Congreve,¹ N. J. Thompson,² and M. A. Baldo¹

¹Department of Electrical Engineering and Computer Science, Massachusetts Institute of Technology, Cambridge, Massachusetts 02139, USA

²Department of Materials Science and Engineering, Massachusetts Institute of Technology, Cambridge, Massachusetts 02139, USA

(Received 10 August 2012; accepted 29 August 2012; published online 12 September 2012)

We demonstrate bilayer organic photovoltaic cells that incorporate a singlet exciton fission sensitizer layer to increase the external quantum efficiency (EQE). This solar cell architecture is realized by pairing the singlet exciton donor layer tris[4-(5-phenylthiophen-2-yl)phenyl]amine (TPTPA) with the singlet exciton fission layer 5,6,11,12-tetraphenylnaphthacene (rubrene). The presence of the rubrene layer at the donor-acceptor interface allows for a singlet generated in TPTPA to undergo singlet exciton fission with a corresponding doubling in the TPTPA EQE from 12.8% to 27.6%. This scheme de-couples singlet exciton fission from photon absorption, exciton diffusion, and charge transport for very high EQE organic photovoltaic cells. © 2012 American Institute of Physics. [<http://dx.doi.org/10.1063/1.4752445>]

Singlet exciton fission is a well-established phenomenon in a small sub-class of organic semiconductors by which a singlet exciton splits into two triplet excitons.¹ The process of singlet exciton fission has recently been proposed as a means to achieve very high external quantum efficiencies (EQE) in organic optoelectronic devices such as photodetectors and photovoltaic cells.²⁻⁴ Although EQEs exceeding 100% have been achieved in organic photodetectors employing singlet exciton fission,² the EQEs have yet to exceed 100% in organic photovoltaic cells (OPVs) utilizing this phenomenon.^{3,4} Due to the limited number of materials that exhibit singlet exciton fission,¹ it is challenging to achieve high photon absorption, long exciton diffusion lengths, efficient charge separation, charge transport, and singlet fission in a single organic semiconductor. In this work, the process of singlet fission is de-coupled from photon absorption, exciton diffusion, and charge transport by inserting a singlet fission material at the donor-acceptor (D-A) interface of an organic photovoltaic cell. Singlet excitons generated in the singlet exciton donor Förster resonance energy transfer (FRET) to the singlet fission material where they undergo singlet fission. This interlayer acts as a singlet fission sensitizer to the singlet donor. In this device structure, the singlet donor can be chosen for high photon absorption, exciton diffusion, and charge transport, and the singlet fission sensitizer can be selected for high singlet fission efficiency to achieve very high EQE organic photovoltaic cells.

In the present work, the singlet donor tris[4-(5-phenylthiophen-2-yl)phenyl]amine⁵ (TPTPA) is sensitized with the singlet fission material 5,6,11,12-tetraphenylnaphthacene⁶ (rubrene). As shown in Fig. 1, the sensitization process begins with the absorption of light by TPTPA, resulting in singlet exciton formation. The singlet exciton then diffuses to the TPTPA-rubrene interface which is then transferred to the singlet state of rubrene by FRET due to the energy alignment of the singlet state of TPTPA ($S_{TPTPA} = 2.8$ eV, esti-

mated from fluorescence) and rubrene ($S_{rubrene} = 2.3$ eV).⁶ The singlet in rubrene then undergoes singlet exciton fission. The process is conditional on the energy of the first excited state being approximately twice the energy of the first triplet ($T_{rubrene} = 1.2$ eV).⁶ If the two triplet excitons are dissociated, one photon absorbed can result in two charge carriers, potentially doubling the EQE in the absorption region of TPTPA. In order to facilitate charge extraction after exciton dissociation, the highest occupied molecular orbital (HOMO) of the singlet fission layer should be equal to or deeper than the singlet donor. In this work, TPTPA and rubrene both have HOMO levels of approximately 5.4 eV.^{7,8}

Before OPV device fabrication, photoluminescence (PL) of a co-deposited film on glass of TPTPA(30%):rubrene(70%), by volume, was measured to characterize energy transfer from TPTPA to rubrene. The absorption coefficients and PL of TPTPA and rubrene are shown in Fig. 2(a). TPTPA absorbs broadly in the region from $350 \text{ nm} < \lambda < 450 \text{ nm}$ while rubrene absorbs light in the region from $450 \text{ nm} < \lambda < 550 \text{ nm}$. Ideally, the singlet donor's absorption peak would be slightly higher in energy than the absorption peak of the singlet fission sensitizer for efficient exciton transfer while maintaining broad solar absorption. To study singlet fission sensitization, TPTPA and rubrene were chosen for non-overlapping absorptions to allow for selective material excitation. When TPTPA is photoexcited ($\lambda = 349 \text{ nm}$) in the co-deposited thin film, TPTPA's fluorescence is fully quenched as singlets on TPTPA are transferred to rubrene as shown in Fig. 2(a).

The process of singlet exciton fission is unaffected by the method of populating singlets (direct photoexcitation versus FRET) in rubrene as shown in Fig. 2(b) by magnetic field dependent change in fluorescence in luminescent thin films. The magnetic field was applied parallel to the film plane. In the co-deposited film, photoexcitation of TPTPA ($\lambda = 365 \text{ nm}$) and subsequent energy transfer to rubrene produces an increase in fluorescence of 19%, and direct photoexcitation of rubrene ($\lambda = 500 \text{ nm}$) produces an increase in fluorescence of 21%. The shapes of these curves with zero crossings at low

^{a)}Electronic mail: reuswig@mit.edu.

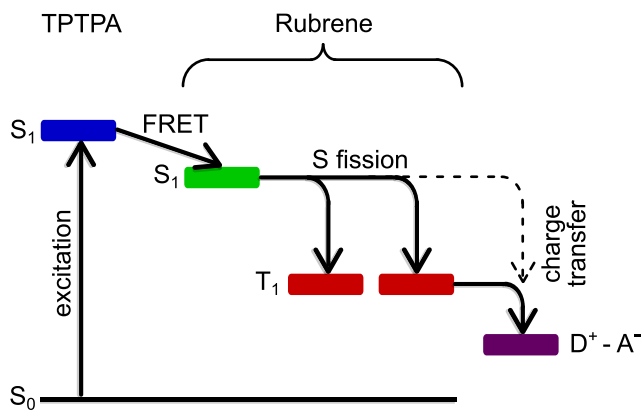


FIG. 1. A schematic representation of singlet fission sensitization scheme in an OPV. Radiation is absorbed by the singlet donor, TPTPA, resulting in singlet generation. The singlet diffuses to the interface and energy transfers to the singlet fission sensitizer layer, rubrene. The singlet on the sensitizer then undergoes singlet exciton fission resulting in two triplets. The triplets then dissociate at the donor-acceptor (D-A) interface resulting in two charge carriers from one photon absorbed in the singlet exciton donor. If the rate of singlet fission is comparable to the rate of singlet charge transfer, direct singlet dissociation (dashed arrow) at the D-A interface may occur.

fields are typical of singlet exciton fission into two triplets.^{6,9} The increase in fluorescence is due to the rate of singlet fission decreasing under high magnetic fields ($H > 0.2$ T) allowing for singlet exciton processes such as fluorescence to compete more efficiently with fission.¹⁰ The measured changes in fluorescence of the co-deposited film are consistent with those of neat rubrene ($\lambda = 500$ nm) [Fig. 2(b)]. Neat TPTPA photoexcited ($\lambda = 365$ nm) under a varying magnetic field, as seen in Fig. 2(b), shows no magnetic field dependent fluorescence. The introduction of magnetic field dependent changes of fluorescence in photoexcited TPTPA demonstrates singlet fission sensitization via exciton energy transfer.

To investigate the effect of singlet fission sensitization in OPVs, we built bilayer heterojunction devices composed of the singlet donor, TPTPA, the singlet fission sensitizer, rubrene, and a perylene diimide (ActivInk N1400 (PDI-CN2), purchased from Polyera) as the electron acceptor. The charge transfer state energy of the OPV must be lower than the triplet energy in the fission material to ensure triplet

dissociation at the D-A interface.¹¹ The electron acceptor was chosen for this reason due to its lowest unoccupied molecular orbital (LUMO) level of 4.3 eV.¹² Devices were fabricated on indium tin oxide (ITO) coated glass substrates. The substrates were cleaned with detergent and solvents and exposed to an O₂-plasma prior to deposition. All organic layers were grown using thermal evaporation under high vacuum ($\sim 10^{-6}$ Torr). The cathode was defined by a 1-mm-diameter shadow mask. The device structure was as follows: ITO (160 nm)/MoO₃ (8 nm)/TPTPA (25 nm)/Rubrene (7 nm)/PDI-CN2 (20 nm)/Bathocuproine (BCP) (7 nm)/Ag (100 nm). The energy level diagram for these devices can be seen in Fig. 3(a).^{7,8,12-14} Control devices without the singlet fission sensitizer interlayer were also grown for comparison.

Current-density-voltage (J - V) curves are shown in Fig. 3(b) for devices with and without fission sensitization layer, performed under AM1.5G illumination (100 mW cm^{-2}). Devices with no fission sensitizer exhibit short-circuit current density $J_{SC} = 0.52 \text{ mA cm}^{-2}$, open-circuit voltage $V_{OC} = 0.49 \text{ V}$, fill factor $FF = 0.53$, and power conversion efficiency $PCE = 0.14\%$. Devices with the rubrene sensitizer layer exhibit $J_{SC} = 0.88 \text{ mA cm}^{-2}$, $V_{OC} = 0.55 \text{ V}$, $FF = 0.59$, and $PCE = 0.29\%$. Similar V_{OC} in the control and sensitized devices indicate the HOMOs of TPTPA and rubrene are close in energy. Also, the FF enhancement indicates no obstruction to charge extraction at the TPTPA-rubrene interface. With the fission sensitizer layer, the J_{SC} and PCE show enhancements of 69% and 107%, respectively, compared to the control devices.

To understand the mechanism of enhancement in J_{SC} , EQE versus wavelength was measured using a xenon lamp with monochromator, a chopper set to $f = 200$ Hz, and a lock-in amplifier. Light intensity was measured using a calibrated silicon photodiode. For EQE measurements at approximate solar operating conditions, the devices were illuminated with a tungsten light source at 50 mW cm^{-2} . EQE curves are shown in Fig. 4 for devices with and without singlet fission sensitization layer. As expected, direct photoexcitation of rubrene adds to the PDI-CN2 photocurrent in the wavelength range of $450 \text{ nm} < \lambda < 550 \text{ nm}$, increasing the EQE in this region from 5.0% to 8.9% when rubrene is

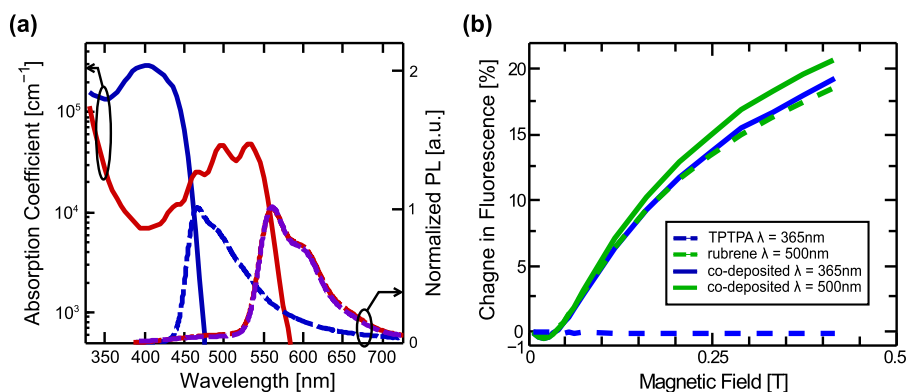


FIG. 2. (a) Absorption coefficient (solid line) and normalized PL (dashed line) photoexcited at $\lambda = 349$ nm of TPTPA (blue) and rubrene (red) thin films. In a co-deposited film of TPTPA(30%):rubrene(70%), TPTPA's fluorescence is fully quenched as singlets are transferred to rubrene (violet). (b) The change in fluorescence under varying applied magnetic fields of photoexcited ($\lambda = 500$ nm) neat rubrene (green dashed line) showing a typical curve of singlet fission to two triplets. Photoexcitation of TPTPA ($\lambda = 365$ nm) and rubrene ($\lambda = 500$ nm) in the ensemble film, the fluorescence increases by 19% (blue solid line) and by 21% (green solid line), respectively, confirming singlet exciton fission. Neat TPTPA, photoexcited at $\lambda = 365$ nm, shows no magnetic field dependent changes in fluorescence (blue dashed line), demonstrating singlet exciton fission sensitization via exciton energy transfer from TPTPA to rubrene.

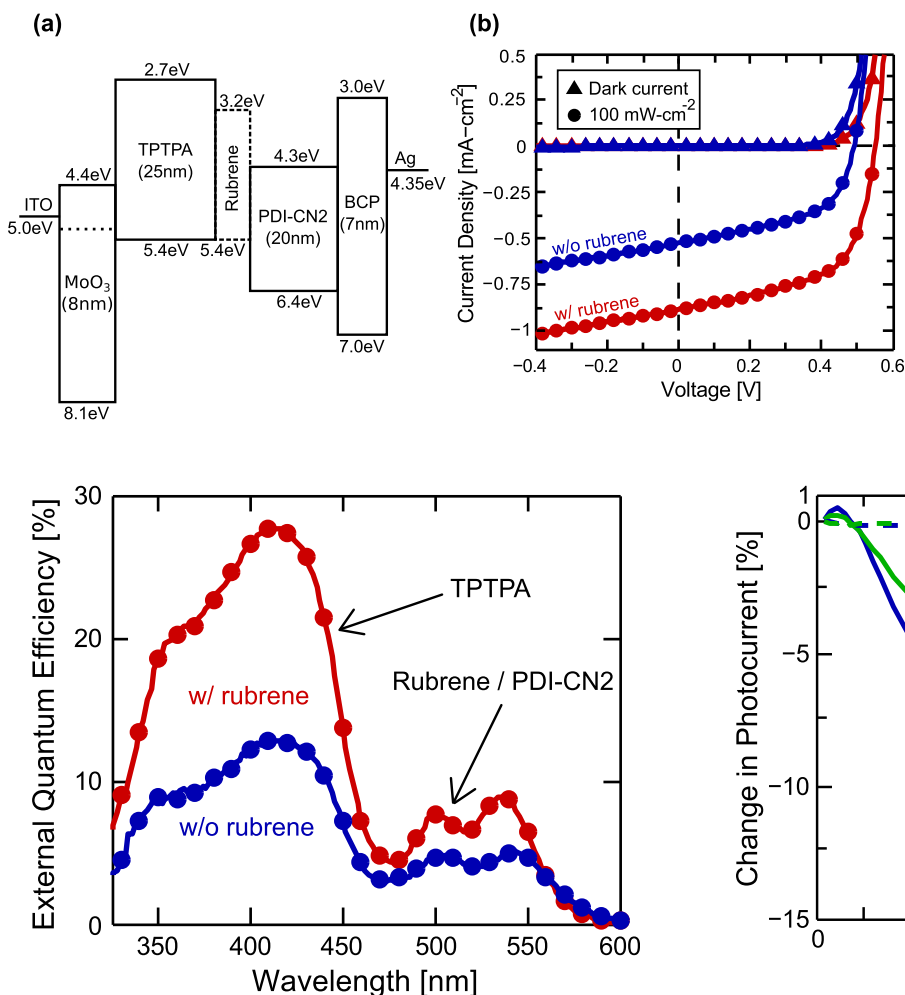


FIG. 4. The measured EQE versus wavelength curves of the OPV device with rubrene (red dots) and without rubrene (blue dots) showing enhancement in the TPTPA region due to singlet fission sensitization via rubrene.

introduced. The EQE in the wavelength range of $350 \text{ nm} < \lambda < 450 \text{ nm}$, associated with TPTPA, exhibits a peak enhancement from 12.8% to 27.6% upon introduction of rubrene.

Although the rubrene interlayer in this work is designed as a singlet fission sensitizer to the singlet donor, TPTPA, it can also act to enhance exciton separation as shown in Refs. 15 and 16. To confirm singlet fission contributes to the enhancement in EQE of the TPTPA region, magnetic field dependent photocurrent measurements were performed, shown in Fig. 5. The magnetic field was applied parallel to the device plane. Photoexcitation of TPTPA ($\lambda = 365 \text{ nm}$) produces a decrease in photocurrent of 14%, because TPTPA singlets undergo energy transfer to rubrene where they are split into triplets. The decrease in photocurrent under high magnetic fields is analogous to the increase in fluorescence shown previously for mixed TPTPA-rubrene films. The magnetic field effect on photocurrent is due to a decrease in the rate of singlet exciton fission under high magnetic fields ($H > 0.2 \text{ T}$). This allows singlet exciton processes such as direct singlet charge transfer, which produces one charge carrier per singlet, to compete more efficiently with singlet exciton fission and triplet charge transfer, which produces two charge carriers per singlet, reducing the observed photo-

FIG. 3. (a) Schematic energy-level diagram and thicknesses of the OPV devices built. The energy-levels are from Refs. 8, 9, and 13–15. (b) The measured dark (triangles) and light (100 mW cm^{-2}) (dots) current-density-voltage (J - V) of the OPV device with rubrene (red) and without rubrene (blue).

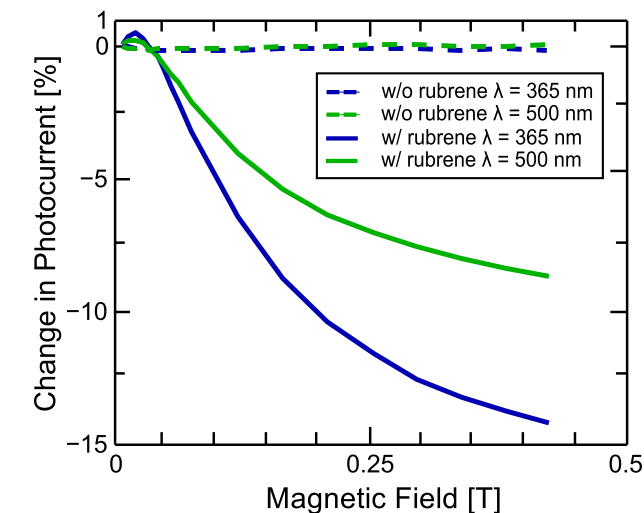


FIG. 5. The change in photocurrent under varying applied magnetic fields at short circuit conditions for OPV with rubrene (solid line) and without rubrene (dashed line) interlayer. For the device with rubrene, the photocurrent decreases by 14% under illumination at $\lambda = 365 \text{ nm}$ (solid blue line) of the TPTPA layer. The photocurrent decreases by 8.7% under illumination at $\lambda = 500 \text{ nm}$ (solid green line) of the rubrene and PDI-CN2 layers. The magnitude of change is smaller due to the PDI-CN2 component of photocurrent being magnetic field independent. In contrast, the device without rubrene shows no magnetic field dependent photocurrent at $\lambda = 365 \text{ nm}$ (dashed blue line) or $\lambda = 500 \text{ nm}$ (dashed green line), confirming singlet exciton fission sensitization of TPTPA via rubrene in an OPV.

current.² Direct photoexcitation of rubrene ($\lambda = 500 \text{ nm}$) produces a decrease in photocurrent of 8.7%. The magnitude of the change is smaller due to competing optical absorption by PDI-CN2 at the same wavelength. The control device without rubrene shows no magnetic field dependent photocurrent in the TPTPA region ($\lambda = 365 \text{ nm}$) or the PDI-CN2 region ($\lambda = 500 \text{ nm}$). The magnetic field dependent photocurrent in the TPTPA region confirms the presence of singlet fission via the rubrene sensitizer layer.

In summary, we have shown an enhancement in EQE in an OPV device due to singlet exciton fission sensitization. The enhancement in peak EQE in the spectral region associated with the singlet exciton donor, TPTPA, increased from 12.8% to 27.6% upon introduction of the rubrene singlet fission sensitization layer. The presence of singlet exciton fission via energy transfer from TPTPA to rubrene was demonstrated in a fluorescent thin film and in a OPV device by magnetic field dependent changes in fluorescence, 19%,

and photocurrent, -14% , respectively. In the device structure introduced here, the singlet donor can be chosen for high photon absorption, long exciton diffusion, and efficient charge transport, and the singlet fission sensitizer can be selected for high singlet exciton fission efficiency for organic photovoltaic cells with EQEs potentially exceeding 100%.

This work was supported as part of the Center for Excitonics, an Energy Frontier Research Center funded by the U.S. Department of Energy, Office of Science, Office of Basic Energy Sciences under Award Number DE-SC0001088 (MIT). D. Congreve was partially supported by the National Science Foundation Graduate Research Fellowship under Grant No. 1122374. Also, we would like to thank Patrick Brown for his help with light and dark J - V measurements.

¹M. Smith and J. Michl, *Chem. Rev.* **110**, 6891 (2010).

²J. Lee, P. Jadhav, and M. Baldo, *Appl. Phys. Lett.* **95**, 033301 (2009).

³P. Jadhav, A. Mohanty, J. Sussman, J. Lee, and M. Baldo, *Nano Lett.* **11**, 1495 (2011).

⁴B. Ehrler, M. Wilson, A. Rao, R. Friend, and N. Greenham, *Nano Lett.* **12**, 1053 (2012).

⁵H. Kageyama, H. Ohishi, M. Tanaka, Y. Ohmori, and Y. Shirota, *Appl. Phys. Lett.* **94**, 063304 (2009).

⁶E. Frankevich, B. Rumyantsev, and V. Lesin, *J. Lumin.* **11**, 91 (1975).

⁷Y. Hamada, H. Kanno, T. Tsujioka, H. Takahashi, and T. Usuki, *Appl. Phys. Lett.* **75**, 1682 (1999).

⁸M. Hirade and C. Adachi, *Appl. Phys. Lett.* **99**, 153302 (2011).

⁹N. Geacintov, M. Pope, and F. Vogel, *Phys. Rev. Lett.* **22**, 593 (1969).

¹⁰R. C. Johnson and R. E. Merrifield, *Phys. Rev. B* **1**, 896 (1970).

¹¹P. Jadhav, P. Brown, N. Thompson, B. Wunsch, A. Mohanty, S. Yost, E. Hontz, T. Van Voorhis, M. Bawendi, V. Bulovic, and M. Baldo, "Triplet exciton dissociation in singlet exciton fission photovoltaics," *Adv. Mater.* (accepted).

¹²X. Zhan, A. Facchetti, S. Barlow, T. J. Marks, M. A. Ratner, M. R. Wasielewski, and S. R. Marder, *Adv. Mater.* **23**, 268–284 (2011).

¹³S. Hammond, J. Meyer, N. Widjonarko, P. Ndione, A. Sigdel, A. Garcia, A. Miedaner, M. Lloyd, A. Kahn, D. Ginley, J. Berry, and D. Olson, *J. Mater. Chem.* **22**, 3249 (2012).

¹⁴A. Kahn, N. Koch, and W. Y. Gao, *J. Polym. Sci., Part B: Polym. Phys.* **41**, 2529 (2003).

¹⁵T. D. Heidel, D. Hochbaum, J. M. Sussman, V. Singh, M. E. Bahlke, I. Hiromi, J. Lee, and M. A. Baldo, *J. Appl. Phys.* **109**, 104502 (2011).

¹⁶C. W. Schlenker, V. S. Barlier, S. W. Chin, M. T. Whited, R. E. McAnally, S. R. Forrest, and M. E. Thompson, *Chem. Mater.* **23**, 4132 (2011).